HHS Public Access

Author manuscript

Nat Neurosci. Author manuscript; available in PMC 2011 November 01.

Published in final edited form as:

Nat Neurosci. 2011 May ; 14(5): 587–594. doi:10.1038/nn.2799.

Structural basis for the role of inhibition in facilitating adult brain plasticity

Jerry L. Chen[1,2], **Walter C. Lin**[1,3], **Jae Won Cha**[4], **Peter T. So**[4,5], **Yoshiyuki Kubota**[6,7,8], and **Elly Nedivi**[1,2,9]

[1]Picower Institute for Learning and Memory, Massachusetts Institute of Technology, Cambridge, Massachusetts, USA.

[2]Department of Biology, Massachusetts Institute of Technology, Cambridge, Massachusetts, USA.

[3]Harvard-MIT Division of Health Science and Technology, Harvard Medical School, Cambridge, Massachusetts, USA.

[4]Department of Mechanical Engineering, Massachusetts Institute of Technology, Cambridge, Massachusetts, USA.

[5]Department of Biological Engineering, Massachusetts Institute of Technology, Cambridge, Massachusetts, USA.

[6]JST, CREST, Maebashi, Japan.

[7]Division of Cerebral Circuitry, National Institute for Physiological Sciences, Okazaki, Japan.

[8]Department of Physiological Science, Graduate University for Advanced Studies (SOKENDAI), Okazaki, Japan.

[9]Deparment of Brain and Cognitive Sciences, Massachusetts Institute of Technology, Cambridge, Massachusetts, USA.

Abstract

While inhibition has been implicated in mediating plasticity in the adult brain, the mechanism remains unclear. Here we present a structural mechanism for the role of inhibition in experience-dependent plasticity. Using chronic *in vivo* two-photon microscopy in the mouse neocortex we show that experience drives structural remodeling of superficial layer 2/3 interneurons in an input- and circuit-specific manner, with up to 16% of branch tips remodeling. Visual deprivation initially induces dendritic branch retractions accompanied by loss of inhibitory inputs onto neighboring pyramidal cells. The resulting decrease in inhibitory tone, also achievable pharmacologically by the antidepressant fluoxetine, provides a permissive environment for further structural adaptation,

Correspondence and requests for materials should be addressed to E.N. (nedivi@mit.edu).

Authors' Contributions J.L.C. and E.N. designed monocular deprivation and binocular deprivation research studies; W.C.L. and E.N. designed fluoxetine research studies; Y.K. performed electron microscopy studies; J.L.C. and W.C.L. performed research and analyzed data; J.W.C and P.T.S. contributed new reagents/analytic tools; J.L.C. and E.N. wrote the paper.

including addition of new synapse bearing branch tips. Our findings suggest that therapeutic approaches that reduce inhibition, when combined with an instructive stimulus, could facilitate restructuring of mature circuits impaired by damage or disease, improving function and perhaps enhancing cognitive abilities.

INTRODUCTION

Promoting plasticity, the ability to adapt, in the adult brain is critically important for enabling functional recovery from disease or injury related neurological damage and for enhancing cognitive abilities such as learning and memory. It is increasingly evident that inhibitory circuits play a key role in neurological deficits as well as experience-dependent plasticity. A variety of genetic disorders that present cognitive deficits, such as autism, Rett and Down syndromes have been associated with excessive inhibition[1–3]. In the case of Down syndrome, reducing inhibition can improve cognitive function[4]. Reducing intracortical inhibition in the visual system, either pharmacologically, through sensory deprivation, or by environmental enrichment has been shown to restore a juvenile state of plasticity in the adult brain[5–8]. Thus, modification of inhibitory circuits could provide an important therapeutic approach. Yet, the mechanism whereby experience alters inhibitory circuitry is unclear, and the extent to which these circuits can be modified in a stimulus- and lamina-specific manner remains unaddressed.

Using a multi-photon microscope system for chronic *in vivo* imaging of neuronal morphology, we previously showed that dendrites of inhibitory interneurons in the adult visual cortex remodel on a day-to-day basis[9]. These remodeling interneurons represent all known interneuron subtypes and reside within a "dynamic zone" corresponding to a superficial strip of layer 2/3 (L2/3)[10]. Electrophysiological studies suggest that the extragranular layers of cortex retain a unique capacity for plasticity that persists beyond development into adulthood[11–13]. We hypothesized that the structural rearrangement of dynamic zone interneurons provides a mechanism for experience-dependent functional plasticity within circuits of the adult cortex. To test this hypothesis we monitored entire dendritic arbors of superficial L2/3 interneurons in the visual cortex of adult mice subjected to monocular deprivation (MD) or binocular deprivation (BD), classic paradigms for investigating experience-dependent plasticity in the visual system.

RESULTS

Monocular Deprivation Increases Branch Tip Dynamics

Adult *thy1-GFP-S* transgenic mice (postnatal day 42–56) expressing GFP in a random subset of neurons sparsely distributed within the superficial cortical layers were surgically implanted with bilateral cranial windows over the visual cortices. Following 3 weeks of recovery, we identified superficial L2/3 interneurons (65–150μm below the pial surface) and acquired a two-photon imaging volume encompassing each cell and its entire dendritic arbor. Cells were imaged weekly while the animal experienced an initial two-week period of normal vision followed by a 14-day MD of the contralateral eye or a 14-day BD, with an intermediate imaging session performed after 4 days of deprivation (Fig. 1a). To ascertain

the location of each cell soma with respect to binocular (V1B) and monocular visual cortex (V1M), we performed optical intrinsic signal imaging after the first two-photon imaging session (Fig. 1b and Supplementary Fig. 1). In addition, at the conclusion of the two-photon imaging time course, we injected a transneuronal tracer, wheat germ agglutinin-Alexa555 (WGA-555) into the ipsilateral eye. We identified the coronal section containing the imaged cell in the fixed brain and confirmed cell depth and location using DAPI staining to visualize cortical laminae, and WGA-555 labeling of thalamacortical projections from the ipsilateral eye to visualize V1B (Fig. 1c).

Ocular dominance plasticity induced by MD in the adult mouse is characterized by a clear potentiation of the non-deprived ipsilateral eye response and by a slight depression of the deprived contralateral eye response[14–18] specific to V1B. More recently, L2/3 interneurons in V1B were shown to exhibit an even stronger ocular dominance shift in response to MD than pyramidal cells largely due to a more robust depression of the deprived eye response[19]. Two-photon imaging of superficial L2/3 interneurons in V1B revealed that under normal vision, 2.98 ± 0.48% (mean ± s.e.m.) of monitored dendritic branch tips remodel per week with 16.7 ± 2.4% of all branch tips remodeling during the entire time course (Fig. 1d–f; 2a,c,d). Each branch tip length change was 8.65 ± 1.40 μm per week or up to 45 μm over the entire time course and included elongations and retractions of existing branch tips as well as the formation and elimination of entire branch tips. MD led to a 3-fold increase in branch tip dynamics compared to normal vision to 9.02 ± 2.01% from 0 to 4 days of MD (0–4d MD) and 8.52 ± 1.70% from 4 to 7 days of MD (4–7d MD) (control versus 0–4d MD, Wilcoxon rank sum test, $p < 0.005$; control versus 4–7d MD, Wilcoxon rank sum test, $p < 0.01$). The increased branch tip dynamics in V1B consisted of a total branch tip length change of 32.7 ± 5.7 μm per cell (Supplementary Fig. 2a). However, MD did not affect the average length change per branch tip (Mann-Whitney *U*-test, $p = 0.96$) .Net arbor size per cell was also unchanged due to a balance of elongations and retractions (Supplementary Fig. 2b). These results suggest that the primary effect of MD on branch tip rearrangements is to increase the number of dynamic branch tips in a manner where overall dendritic length is preserved. The 7 days of increased branch tip dynamics after MD coincides with the time required for a functional ocular dominance shift to occur in the adult mouse[14–18]. MD beyond 7 days does not elicit a further ocular dominance shift[17]. Correspondingly, we found that branch tip dynamics decreased below baseline levels from 7 to 14 days of MD (control versus 7–14d MD, Wilcoxon rank sum test, $p < 0.05$).

Branch tip dynamics in superficial L2/3 interneurons of V1M during normal vision was 3.15 ± 0.61% per week, comparable to that in V1B (Fig. 2b, c). MD led to an initial decrease in branch tip dynamics from 0–4d MD (control versus 0–4d MD, Wilcoxon rank sum test, $p < 0.05$). However, branch tip dynamics returned to baseline rates from 4–7d MD and 7–14d MD (control versus 4–7d MD, Wilcoxon rank sum test, $p = 0.39$; control versus 7–14d MD, Wilcoxon rank sum test, $p = 0.07$). These findings demonstrate that increased interneuron branch dynamics induced by MD are specific to V1B where MD induces an ocular dominance shift, and do not occur in V1M in response to the same stimulus.

To confirm that interneuron dendritic branch tip remodeling reflects changes in synaptic input, we performed electron microscopy on a newly extended branch tip imaged *in vivo*.

Immediately after the final imaging session, brains were fixed and a dendrite containing a newly elongated branch tip 7 μm long was relocated and stained with anti-GFP DAB (Fig. 3a–c). Serial electron microscopy reconstruction of the very distal tip of the elongated region revealed 3 (putatively excitatory) synaptic contacts clustered within a 2.3 μm stretch of dendrite (Fig. 3d, e). In comparison, reconstruction of a 13.7μm portion of the stable dendrite proximal to the elongated branch tip indicated 6 (putatively excitatory) synaptic contacts (Fig. 3d, f). These results indicate that synapses are formed on new branch tips and that the synaptic density of these new regions is comparable to that of stable regions.

Branch Tip Dynamics are Stimulus and Lamina-Specific

In the non-human primate visual system, superficial L2/3 has been identified as a region where bottom-up feedforward inputs[20] converge with top-down feedback inputs modulating attention, response strength, and saliency[21,22]. The presence of similar anatomical pathways in the mouse visual cortex[23–25] and the laminar restriction of interneuron dendritic remodeling to superficial L2/3[10] led us to propose that inhibitory circuit restructuring specifically in this locale serves to coordinate the relative contribution of these two visual processing pathways. To test this hypothesis, we explored whether MD, which directly and selectively alters the feedforward pathway, affects branch tip dynamics in a spatially-restricted manner that reflects pathway-specific rewiring. We examined the position of dynamic branch tips before and during the first 7 days of MD in V1B with respect to laminar location (Fig. 4a). Under normal vision, branch tip elongations were distributed with 63% in L1 (0–65μm below the pial surface), an area dominated by feedback input, and 37% in superficial L2/3 (65–150μm), a location more strongly influenced by feedforward thalamic input (Fig. 4b). Branch tip retractions were distributed with 54% in L1 and 46% in superficial L2/3. At 0–4d MD, this distribution changed dramatically such that 88% of branch tip retractions occur within L2/3 (control retraction versus 0–4d MD retractions, K-S test, $p < 0.05$). Closer analysis of branch tip dynamics by layer shows that in L2/3, MD led to an initial increase in branch tip retractions from 0–4d MD followed by an increase in elongations from 4–7d MD (Fig. 4c; Wilcoxon rank sum test, control versus 0–4d MD elongations, $p < 0.01$; Wilcoxon rank sum test, control versus 4–7d MD elongations: $p < 0.05$). In L1, only a brief increase in retractions was observed at 4–7d MD (control versus 4–7d MD retractions, Wilcoxon rank sum test, $p < 0.05$). By comparison, elongations and retractions remain balanced in L2/3 of V1M during MD (Supplementary Fig. 3) (0–4d MD elongations versus retractions Wilcoxon rank sum test, $p = 0.69$; 4–7d MD elongations versus retractions Wilcoxon rank sum test, $p = 0.24$). These results demonstrate that in response to experience, superficial L2/3 interneurons of binocular visual cortex are capable of selectively re-distributing branch tips that are potentially receiving different inputs, visually-driven feedforward inputs in L2/3 or top-down inputs in L1.

BD as a visual manipulation distinct from MD has proven insightful in distinguishing between the role of sensory deprivation and sensory experience during experience-dependent plasticity[17,26–28]. To determine the experience-dependent features of interneuron dendritic remodeling in V1B, we compared MD-induced branch tip dynamics to those in animals subjected to a 14 day BD. Overall, BD in V1B did not significantly increase the rate of branch tip remodeling in superficial L2/3 interneurons (Fig. 5a, repeated measures

ANOVA, $p = 0.28$). However, analysis by layer shows reduced elongations from 0 to 4 days of BD and reduced retractions from 4 to 7 days of BD for branch tips in L1 (Fig. 5b, control versus 0–4d BD elongations, Wilcoxon rank sum test, $p < 0.05$; control versus 4–7d BD retractions, Wilcoxon rank sum test, $p < 0.05$). For branch tips in L2/3, BD led to an increase in retractions from 0–4d BD similar to that observed from 0–4d MD (control versus 0–4d BD retractions, Wilcoxon rank sum test, $p < 0.05$). In contrast to increased branch tip elongations seen in this layer between 4–7d MD, we observed further retractions between 4–7d BD (control versus 4–7d BD retractions, Wilcoxon rank sum test, $p < 0.02$). These findings support the idea that branch tip remodeling in L2/3 specifically reflects changes in sensory input and that retractions observed in L2/3 during MD and BD in binocular visual cortex represent a deprivation-induced response. Furthermore, it suggests that the elongations in L2/3 of V1B from 4–7d MD require sensory experience from the non-deprived eye.

Since approximately 80% of synapses on interneuron dendrites are excitatory (Y. Kubota et al., *Soc. Neurosci. Abstr*. 470.20, 2007), the primary effect of branch tip retractions elicited by sensory deprivation during both MD and BD would likely be loss of excitatory input, resulting in reduced inhibition within the local circuit. To determine if the loss of excitatory input in response to MD is limited to dynamic branch tips or also occurs on stable arbors we performed immunohistochemistry on GFP-labeled superficial L2/3 interneurons in V1B using vesicular glutamate transporter 1 (VGlut1) to stain for excitatory pre-synaptic terminals impinging upon dendritic branch segments (Supplementary Fig. 4). We did not find a significant decrease in excitatory synapse density in animals experiencing 4 days of MD (control versus 4d MD, Mann-Whitney *U*-test, $p = 0.26$), suggesting that sensory deprivation does not produce detectable excitatory synapse loss on stable interneuron dendrites, only loss of input due to eliminated dendrites.

Deprivation-Induced Inhibitory Input Loss on L5 Dendrites

We next asked whether the loss of excitatory input on retracting branch tips could sufficiently impact interneuron activity as to reduce inhibition within the local circuit. To address this question, we examined axonal boutons of the same L2/3 interneurons in V1B where branch tip retractions were observed during the first 4 days of MD (Fig. 6a). During 2 weeks of normal vision, $2.54 \pm 0.66\%$ and $2.79 \pm 1.75\%$ of boutons on these cells were added or eliminated respectively (Fig. 6b). From 0–4d MD, the fraction of bouton additions decreased to $0.70 \pm 0.37\%$ (control versus 0–4d MD additions, Wilcoxon rank sum test, $p < 0.05$) while the fraction of eliminations increased to $7.63 \pm 2.16\%$ (control versus 0–4d MD eliminations, Wilcoxon rank sum test, $p < 0.001$). These results demonstrate that deprivation-induced retractions of interneuron dendrites are accompanied by bouton loss from axons of the same cells.

Axons of L2/3 interneurons synapse locally onto dendrites and soma of L2/3 pyramidal neurons as well as the apical dendrites of L5 pyramidal neurons[29]. To determine if the bouton retractions of L2/3 interneurons seen in response to MD are mirrored by elimination of inhibitory synapses on excitatory cell types in their vicinity, we performed immunohistochemistry for vesicular GABA transporter (VGAT), a marker for inhibitory

pre-synaptic terminals[30], on GFP-labeled L2/3 and L5 pyramidal neurons. Antibody staining for VGAT in V1B revealed punctate staining of inhibitory synapses on the soma and dendrites of L2/3 pyramidal neurons as well as the apical dendrites of L5 pyramidal neurons extending into L2/3 (Fig. 6c). Four days of MD did not affect the number of perisomatic or dendritic synapses on L2/3 pyramidal neurons (Fig. 6d). Interestingly, inhibitory synapse density on L5 apical dendrites significantly decreased from 4.42 ± 0.48 to 2.70 ± 0.41 synapses per 10 μm of dendrite (control versus 4d MD, Mann-Whitney *U*-test, $p < 0.05$). These findings demonstrate that during MD, dendritic branch tip retractions in superficial L2/3 interneurons occur concurrently with the selective elimination of inhibitory input onto the apical dendrites of L5 pyramidal neurons.

Fluoxetine Increases Interneuron Branch Tip Dynamics

It was previously shown that the widely used anti-depressant drug, fluoxetine, can reduce intracortical inhibition and restore a juvenile level of ocular dominance plasticity in the adult rodent visual cortex[7]. To further examine the role of intracortical inhibition in promoting visual cortical plasticity in the adult, we measured interneuron branch tip dynamics in V1B in animals receiving fluoxetine for 3-weeks at a dosage previously shown to reduce cortical extracellular GABA. We then performed a brief 4d MD sufficient to induce an ocular dominance shift while the animals continued to receive fluoxetine (Fig. 7a). Under normal visual experience, fluoxetine treatment led to an increase in overall branch tip dynamics compared to control conditions (Fig. 7b, c; control versus fluoxetine, Wilcoxon rank sum test, $p < 0.02$). These increased dynamics applied to both elongations and retractions in L1 and L2/3 (Fig. 7c), suggesting that pharmacological reduction of intracortical inhibition by fluoxetine can promote structural remodeling in the adult brain. Interestingly, similar to visual perturbations such as MD and BD, fluoxetine promotes remodeling of existing branch tips as opposed to the addition or elimination of entire branch tips (Supplementary Fig. 5a, b), suggesting that visual deprivations and fluoxetine may act through a common mechanism.

Fluoxetine in combination with a brief 4d MD led to an immediate increase in elongations in L2/3 (elongations versus retractions, Wilcoxon rank sum test, $p < 0.05$; fluoxetine versus 0–4d MD with fluoxetine, Wilcoxon rank sum test, $p < 0.05$). These increased elongations were similar to those observed during 4–7d MD without fluoxetine (0–4d MD versus 0–4d MD with fluoxetine, Mann-Whitney *U*-test, $p < 0.01$; 4–7d MD versus 0–4d MD with fluoxetine, Mann-Whitney *U*-test, $p = 0.62$) and specifically occurred during the first two days of MD (Supplementary Fig. 5c). This time course of branch tip dynamics seen with fluoxetine treatment, suggests that reduction of intracortical inhibition by fluoxetine can replace the initial period of deprivation-induced disinhibition in enabling L2/3 branch tip elongations to occur.

DISCUSSION

While inhibition has been implicated in mediating plasticity in the adult brain[6–8,31], the mechanism has been unclear. Our findings suggest that structural remodeling of superficial

L2/3 interneurons in an input-specific manner can sculpt mature inhibitory circuits so as to facilitate or attenuate experience-dependent plasticity.

Deprivation-Induced Branch Tip Retractions in Interneurons

It is becoming increasingly apparent that MD- induced ocular dominance plasticity produces different responses in inhibitory neurons as compared to excitatory neurons. During development, L2/3 inhibitory neurons exhibit a delayed ocular dominance plasticity compared to excitatory neurons in the same layer[32]. In the adult, ocular dominance plasticity in excitatory neurons lacks the strong depression of the deprived eye response, and is mostly comprised of potentiation of the non-deprived eye response[19]. This is accompanied by an increase rather than loss of dendritic spines on excitatory cells, representing gain of excitatory synapses[16]. We find that MD triggers an initial increase in L2/3 interneuron branch retractions together with elimination of inhibitory boutons targeting the apical dendrites of L5 pyramidal neurons. These structural changes occur concomitant with the strong depression of deprived eye response reported in these interneurons[19]. The increased L2/3 branch tip retractions in interneurons during MD are specific to V1B, a region where contralateral and ipsilateral eye inputs converge. Binocular deprivation can also promote retractions suggesting that this response is primarily deprivation-induced. While V1M during MD and V1B during BD both experience a complete loss of visual activity, the lack of increased L2/3 retractions in V1M during MD, suggests that the competitive presence of the ipsilateral eye pathway is required for the retractions seen in V1B between 0–4d MD.

Deprivation-induced retractions of interneuron dendrites were not accompanied by a deprivation-induced decrease in excitatory synapses on stable arbors when assayed immunohistochemically. While we cannot exclude the possibility of weight changes on non-remodeling synapses, these findings suggests that deprivation-induced changes in excitatory drive to L2/3 interneurons may potentially be restricted to remodeling branches.

Functional Consequences of Interneuron Branch Tip Changes

Can changes in synaptic numbers associated with interneuron branch tip remodeling in and of itself be sufficient to alter neuron and circuit function? We find that MD in V1B produces a total branch tip length change of 32.7 ± 5.7 μm per cell or 1.81 ± 0.31% of the total branch tip length per cell. Measurements by electron microscopy have indicated that the synaptic density of L2/3 interneuron dendrites is approximately 1 synapse per μm (Y. Kubota et al., *Soc. Neurosci. Abstr*. 470.20, 2007). We estimate that the synaptic turnover associated with these structural rearrangements during MD is on the order of ~30 synapses per cell with approximately 10% of branch tips remodeling.

About 80% of the synapses on distal interneuron dendrites represent excitatory inputs (Y. Kubota et al., *Soc. Neurosci. Abstr*. 470.20, 2007) from a large number of local pyramidal neurons that each contributes only (3–7) synapses[33]. It is estimated that as few as 10 pre-synaptic, temporally correlated excitatory inputs are sufficient to trigger an action potential in inhibitory cells[34]. For bitufted interneurons, a train of action potentials from even a single synaptic contact can produce an action potential[35]. Thus, a total branch tip length change of

~30 μm (or ~30 synapses) per cell could potentially alter the connectivity of 5–10 excitatory pre-synaptic partners, each with significant ability to initiate interneuron firing.

One inhibitory cell makes a large number (15–20) of synapses onto local excitatory cells despite representing only about 20% of cortical neurons. As a result, the activity of a given post-synaptic cell can be more strongly influenced by the minority of inhibitory neurons that synapse onto it than by its excitatory inputs. We show that dendritic retractions during the first four days of MD are accompanied by bouton loss from axons of the same imaged interneurons, demonstrating that experience eliciting structural changes that reduce drive to these cells also elicits changes that reduce output.

It has been proposed that structural plasticity in the adult brain serves to increase the number of potential synaptic contacts by increasing spatial access to distinct circuits within an arbor's vicinity[36]. For example, it is estimated that the geometry and space occupied by each dendritic spine in mouse cortex is capable of making approximately 4 potential synaptic contacts[37]. An entire dendritic branch tip likely contains an even higher number of possible synaptic connections considering its shape and observed changes in length. By the same rationale, increasing an interneuron's potential for sampling distinct circuits would be more readily achieved by modest length changes in several branch tips spatially distributed throughout the dendritic field as compared to a substantial length change of a single branch tip. We found that the average length change per branch tip was unaffected by MD while the fraction of individual dynamic branch tips per cell increased by ~2 fold. Since MD primarily acts to increases the number of dynamic branch tips per cell, our data would suggest that interneuron dendritic arbor remodeling may function to access and alter connectivity between different circuits in cortical space. The relative number of synapses lost or gained during a branch tip retraction or elongation may not be as important as the change to the circuit diagram resulting from the shuffling of synaptic partners. The cell type and laminar-specificity of both pre- and post-synaptic structural dynamics argue that the partner sampling occurring during synaptic remodeling is circuit specific.

Disinhibition as a Mechanism of Adult Plasticity

Given the predominance of excitatory synapses on interneuron dendrites, we propose that the initial branch tip retractions induced by 4 days of BD or MD results in reducing the contribution of excitatory drive to interneurons, producing a period of disinhibition in the local circuit (Supplementary Fig. 6). Loss of visual input in one eye through lid suture, enucleation, or tetrodotoxin injection has been shown to reduce expression of GABA, GABA receptor, and the GABA synthesizing enzyme, glutamate decarboxylase, specifically in the deprived-eye column in the adult monkey visual cortex[38–41]. Consistent with these studies, we find that interneuron branch tip retractions are accompanied by the loss of inhibitory axonal boutons during the same period. Moreover, we find that elimination of these pre-synaptic terminals occurs concurrently with the loss of inhibitory synapses onto apical dendrites of L5 pyramidal neurons. While we don't know that inhibitory synapse loss on L5 pyramidal apical dendrites are from L2/3 interneurons, given that these interneuron's projections are local, they most likely are. Interestingly, MD has been shown to specifically increase dendritic spine formation in L5, but not L2/3, pyramidal neurons[16]. Our findings

provide additional evidence that L5 pyramidal neurons have a unique propensity for experience-dependent remodeling of both excitatory (as inferred by dendritic spine changes) and inhibitory inputs during ocular dominance plasticity. We propose that the loss of inhibitory input enables the formation of dendritic spines that represent the strengthening of non-deprived eye input to these cells potentially enabled by an increase in spike-timing dependent plasticity wherein the reduced inhibitory tone facilitates the induction of synaptic potentiation[42]. Further, disinhibition within the circuit may also enable the increased L2/3 interneuron branch tip elongations observed from 4 to 7 days of MD, contingent on visual input from the non-deprived eye.

In support of the relationship between branch tip retraction and disinhibition, we demonstrate that global disinhibition induced by fluoxetine treatment[7] can provide a permissive environment similar to that afforded by sensory deprivation. Fluoxetine treatment during normal vision enhanced structural dynamics. When this disinhibition was paired with a brief MD it allowed the immediate strengthening of non-deprived eye connections, including branch tip elongations, resulting in a faster ocular dominance shift. The maturation of inhibitory circuits during development has been demonstrated to regulate the onset and closure of critical period plasticity[43–45]. One of the fundamental differences between critical period and adult plasticity in the mouse visual cortex is the duration of MD required to produce an ocular dominance shift[15,17,18]. The time necessary for visual deprivation to produce the initial branch tip retractions and local disinhibition of mature interneurons may be a contributing factor to the prolonged MD required for adult ocular dominance plasticity.

The consequence of strengthening non-deprived eye input onto both pyramidal neurons and interneurons would be reestablishment of excitatory drive onto these interneurons, thus restoring inhibition to the local circuit. Similar to what has been observed in the auditory cortex[31], this rebalancing of excitation/inhibition may bring the window of plasticity afforded by disinhibition to a close, contributing to the saturation in both structural and ocular dominance plasticity observed after 7d MD. In this respect, the plasticity of L2/3 interneurons serves as a form of homeostatic regulation, triggering both the beginning and end of functional as well as structural adaptation in this circuit.

Conclusions

Our findings support a role for disinhibition in experience-dependent plasticity and provide a potential structural mechanism that would facilitate circuit-specific modifications. They further suggest that therapeutic approaches that reduce cortical inhibition are effective only in combination with an instructive stimulus. While fluoxetine treatment does not afford the same circuit-specific disinhibition as deprivation, with appropriately selective input it could nevertheless prove effective in enhancing cognitive abilities and restoring function to fully developed circuits impaired by neurological damage or disease.

METHODS

All animal work was approved by the Massachusetts Institute of Technology Committee on Animal Care and conforms to National Institutes of Health guidelines for the use and care of vertebrate animals.

Surgical Procedure and Fluoxetine Administration

To allow long-term visualization of *in vivo* neuronal morphology cranial windows were bilaterally implanted over the visual cortices of adult *thy1*-GFP-S mice (postnatal days 42–57) as previously described[10]. Animals were housed singly for the remainder of the experiment. Sulfamethoxazole (1 mg/ml) and trimethoprim (0.2 mg/ml) were chronically administered in the drinking water through the final imaging session to maintain optical clarity of implanted windows. For animals subjected to fluoxetine treatment, fluoxetine-hydrochloride (160 mg/L) was chronically administered in the drinking water with Sulfamethoxazole (6 mg/tablet) and Trimethoprim (1 mg/tablet) supplemented in the food pellet (Bio-Serv).

Two-Photon Imaging

Starting at three weeks after cranial window surgery, allowing sufficient time for recovery, adult mice were anesthetized with 1.25% avertin (7.5 ml/kg IP). Anaesthesia was monitored by breathing rate and foot pinch reflex and additional doses of anaesthetic were administered during the imaging session as needed. *In vivo* two-photon imaging was performed using a custom-built microscope modified for *in vivo* imaging by including a custom-made stereotaxic restraint affixed to a stage insert and custom acquisition software. The light source for two-photon excitation was a commercial Mai Tai HP Ti:Sapphire laser (Spectra-Physics) pumped by a 14-W solid state laser delivering 100 fs pulses at a rate of 80 MHz with the power delivered to the objective ranging from approximately 37–50 mW depending on imaging depth. Z-resolution was obtained with a piezo actuator positioning system (Piezosystem Jena) mounted to the objective. The excitation wavelength was set to 950 nm, with the excitation signal passing through a 20×/1.0 NA water immersion objective (Plan-Apochromat, Zeiss) and collected after a barrier filter by a photomultiplier tube. Given the sparse density of GFP expression in the *thy1*-GFP-S line, typically only one cell (with a maximum of two) was imaged per animal. Interneurons are initially identified based on their complex, local dendritic arborization, lack of apical dendrite, small diameter dendritic processes, and general absence or sparseness of dendritic spines.

Optical Intrinsic Signal Imaging

For functional identification of monocular and V1B, optical imaging of intrinsic signal and data analysis were performed as described previously [46]. Mice were anesthetized and maintained on 0.5–0.8% isofluorane supplemented by chloroprothixene (10 mg/kg, i.m.), and placed in a stereotaxic frame. The heart rate was continuously monitored through electrocardiograph leads attached to the animal. For visual stimuli, a horizontal bar (5° in height and 73° in width) drifting up with a period of 12 seconds was presented for 60 cycles on a high-refresh-rate monitor positioned 25 cm in front of the animal. Optical images of visual cortex were acquired continuously under a 610 nm illumination with an intrinsic

imaging system (LongDaq Imager 3001/C; Optical Imaging Inc.) and a 2.5×/0.075 NA (Zeiss) objective. Images were spatially binned by 4×4 pixels for analysis. Cortical intrinsic signal was obtained by extracting the Fourier component of light reflectance changes matched to the stimulus frequency whereby the magnitudes of response in these maps are fractional changes in reflectance. The magnitude maps were thresholded at 30% of peak response amplitude to define a response region. Primary visual cortex was determined by stimulation of both eyes. V1B was determined by stimulation of the ipsilateral eye. Monocular visual cortex was determined by subtracting the map of V1B from the map of primary visual cortex.

Measurement of Ocular Dominance

Ocular dominance during normal conditions and after monocular deprivation was determined from optical intrinsic signal images as previously described[17]. The ocular dominance index (ODI) was calculated from the average of $(C - I)/(C + I)$ for all pixels in the region identified as binocular visual cortex, where C and I represent the response magnitude of each pixel to the contralateral and ipsilateral eyes, respectively. The ODI ranges from +1 to −1, where a positive value indicates a contralateral bias, and a negative value an ipsilateral bias.

Monocular and Binocular Deprivation

Monocular and binocular deprivation were performed by eyelid suture. Mice were anesthetized by 1.25% avertin (7.5 ml/kg IP). Lid margins were trimmed and triple antibiotic ophthalmic ointment (Bausch & Lomb) was applied to the eye. Three to five mattress stitches were placed using 6–0 vicryl along the extent of the trimmed lids. Suture integrity was inspected directly prior to each imaging session. Animals whose eyelids did not seal fully shut or had reopened were excluded from further experiments.

Transneuronal Labeling of Thalamacortical Projections

Wheat germ agglutinin-Alexa555 conjugate (100mg/mL, 2–3 μl; Molecular Probes) in saline was injected into the ipsilateral eye. After 3–5 d post-injection, animals were anesthetized with 1.25% avertin (7.5 ml/kg IP) and perfused transcardially with 4% paraformaldehyde (PFA) in phosphate buffer, pH 7.4. The brain was extracted and fixed overnight in 4% PFA. Seventy-five micrometer-thick coronal sections were cut from the visual cortex using a vibratome (Leica VT100; Leica). Sections were subsequently incubated with 4’6-diamidino-2-phenylindole (DAPI) (1:1,000; Sigma) before mounting and visualization. Imaged cells were identified by location, morphology, and local landmarks. Images were acquired with an upright epi-fluorescence scope using a 1×/0.04 NA, 10×/0.30 NA, or 20 ×/0.75 NA objective (Nikon).

Immunohistochemistry

Brains were processed for immunohistochemistry essentially as described[47]. Boundaries for V1B were marked with penetrations of DiD (Invitrogen) based on maps obtained with optical intrinsic imaging. Sections were first incubated with GFP (rat monoclonal antibody; 1:1000; Nacalai) in addition to VGAT (rabbit polyclonal antibody; 1:1000; Synaptic

Systems) or VGlut1 (guinea pig polyclonal; 1:1000; Synaptic Systems) followed with appropriate Alexa488 and 555-conjugated goat IgG secondary antibodies (1:400; Molecular Probes). Images were acquired with a custom two-photon microscope, a Fluoview confocal (Olympus, Tokyo, Japan) or an upright epi-fluorescence scope (Nikon, Tokyo, Japan) using a 203/N.A. 0.5 (Olympus), 203/N.A. 0.75 (Nikon), or 403/N.A.1.30 (Nikon) objective.

Immunoelectron Microscopy

For post-hoc localization of previously *in vivo* imaged dendrites, blood vessels were labeled with a tail vein injection of fixable rhodamine dextran (5% in PBS, 50uL; Sigma) delivered 30 minutes prior to perfusion. Animals were fixed and perfused with an initial solution of 250 mM sucrose, 5 mM $MgCl_2$ in 0.02 M phosphate buffer (PB; pH 7.4) followed by 4% paraformaldehyde containing 0.2% picric acid and 0.5% glutaraldehyde in 0.1 M PB. Following perfusion and fixation, cranial windows were removed and penetrations of DiD (Invitrogen) were made into cortex around the imaged region. Brains were removed and 50μm thin sections were cut parallel to the imaging plane. Brain sections were visualized with an epifluorescence microscope. The brain section containing the branch tip of interest was identified by combining *in vivo* two-photon images and blood vessel maps with post-hoc blood vessel labeling and DiD penetrations. The identified section was prepared for immuno electron microscopy as previously described[48]. Imaged dendrites were stained by immunohistochemistry using a rabbit antiserum against eGFP (1: 2000; kind gift from Dr Nobuaki Tamamaki, Kumamoto University, Japan). The neurons were labeled with nickel-diaminobenzidine (DAB). Prepared sections were then either serially re-sectioned at thickness settings 50 nm using an ultramicrotome (Reichert Ultracut S, Leica Microsystems, Wetzlar, Germany) and imaged using TEM (Hitachi H-7000 equipped with AMT CCD camera XR-41, Hitachi, Japan), or milled at 30 nm pitch and serially imaged using FIB-SEM CrossBeam Workstation (Carl Zeiss NVision40, Oberkochen, Germany). Image reconstruction and analysis was performed with Reconstruction (http://synapses.clm.utexas.edu/tools/index.stm).

Data and Statistical Analysis

Using Matlab (Mathworks) and ImageJ (National Institutes of Health), 16-bit two-photon raw scanner data was converted into an 8-bit image z-stack. For each individual cell, 4-D (x, y, z, and t) stacks were manually traced in Neurolucida (MicroBrightField, Inc.) and analyzed blind to age. branch tips (segments of dendrite from the last branch point to the terminal) with terminals that could be confidently identified across all imaging sessions, not extending beyond the imaging volume, or obscured by blood vessels were monitored and included in analysis. For unbiased identification of dynamic branch tips, a Fano Factor (FF) value was calculated for each branch tip based on branch tip length measurements obtained from Neurolucida across all imaging sessions. The FF has been previously shown to be the most accurate measure of branch dynamics as confirmed by visual inspection and robustly identifies small branch tip changes while accounting for variability during imaging or manual reconstructions[10]. Monitored branch tips with FF>1.09, representing the 1.5*interquartile range above the upper quartile of the sample population were identified, confirmed as dynamic by visual examination, and subjected to further analysis. The mean FF across all monitored branch tips for each superficial L2/3 interneuron was calculated to

confirm that each cell met the threshold (mean FF>0.35) previously determined for a dynamic cell. In total, 1662 monitored dendritic branch tips out of 1728 total branch tips from 53 cells from 50 animals were followed over 6–7 imaging sessions.

For each cell, the percentage of branch tips elongating or retracting between two successive imaging sessions relative to the total branch tip number of the previous imaging session, were defined as the rates of branch tip elongations and retractions, respectively. Elongations and retractions included both the elongations and retractions of existing branch tips as well as the addition and elimination of entire branch tips. Rate of branch tip dynamics was defined as the sum of the rates of branch tip elongations and retractions. For all imaging intervals, rates of branch tip dynamics were normalized to a '% per week' unit by calculating the percent of dynamic branch tips, multiplied by 7, divided by the number of days between imaging sessions. The depth of each dynamic branch tip was determined from analysis of the imaging volume data in Neuroleucida based on its position relative to the soma, with the soma depth measured by z-stack position relative to the pial surface and verified by post-hoc DAPI staining showing the L1–L2/3 border at ~65um below the pial surface. For bouton analysis, only proximal axonal arbors emanating from the soma of the imaged cell were analyzed. Bouton analysis was performed as previously described[49]. Briefly, boutons were identified as varicosities that were at least three times brighter than neighboring axonal segments and persisted for at least two consecutive imaging sessions. Bouton elimination was scored when varicosity luminosity dropped to 1.3 times below backbone brightness and persisted for at least two consecutive imaging sessions. Wilcoxon rank sum test, Mann-Whitney *U*-test, or repeated measures ANOVA were used for statistical analysis of time course data where *n* indicate the number of cells. K-S test was used for statistical analysis of laminar distribution of dynamic branch tips where *n* indicates the number of branch tips. All error bars are s.e.m.

Supplementary Material

Refer to Web version on PubMed Central for supplementary material.

Acknowledgements

We thank J. Leslie, R. Schecter, and J. Hoch for comments on the manuscript; M.F. Bear for helpful discussions; M. Kozberg for assistance in data analysis; J. Coleman, H.B. Yu, S. Horng, and C. McCurry for assistance with optical intrinsic imaging; Y. Yamamoto (Yokohama Demonstration Laboratory, SII NanoTecnnology Inc.) for data collection assistance by Zeiss NVision40; and S. Hata and H. Kita (NIPS) for serial EM reconstruction. This work was sponsored by grants to E.N. from the National Eye Institute (R01 EY017656) and from the Stanley Center for Psychiatric Research. J.L.C. was supported in part by the MIT-Portugal program. J.W.C. was supported in part by the Singapore-MIT Alliance-2 and Singapore-MIT Alliance for Research and Technology. Y.K. was supposed by grant-in-aid for scientific research from the Ministry of Education, Culture, Sports, Science and Technology of Japan (20500300, 22120518).

REFERENCES

1. Rubenstein JL, Merzenich MM. Model of autism: increased ratio of excitation/inhibition in key neural systems. Genes Brain Behav. 2003; 2:255–267. [PubMed: 14606691]
2. Dani VS, et al. Reduced cortical activity due to a shift in the balance between excitation and inhibition in a mouse model of Rett syndrome. Proc Natl Acad Sci U S A. 2005; 102:12560–12565. [PubMed: 16116096]

3. Kleschevnikov AM, et al. Hippocampal long-term potentiation suppressed by increased inhibition in the Ts65Dn mouse, a genetic model of Down syndrome. J Neurosci. 2004; 24:8153–8160. [PubMed: 15371516]
4. Fernandez F, et al. Pharmacotherapy for cognitive impairment in a mouse model of Down syndrome. Nat Neurosci. 2007; 10:411–413. [PubMed: 17322876]
5. Harauzov A, et al. Reducing intracortical inhibition in the adult visual cortex promotes ocular dominance plasticity. J Neurosci. 2010; 30:361–371. [PubMed: 20053917]
6. He HY, Hodos W, Quinlan EM. Visual deprivation reactivates rapid ocular dominance plasticity in adult visual cortex. J Neurosci. 2006; 26:2951–2955. [PubMed: 16540572]
7. Maya Vetencourt JF, et al. The antidepressant fluoxetine restores plasticity in the adult visual cortex. Science. 2008; 320:385–388. [PubMed: 18420937]
8. Sale A, et al. Environmental enrichment in adulthood promotes amblyopia recovery through a reduction of intracortical inhibition. Nat Neurosci. 2007; 10:679–681. [PubMed: 17468749]
9. Lee WC, et al. Dynamic remodeling of dendritic arbors in GABAergic interneurons of adult visual cortex. PLoS Biol. 2006; 4:e29. [PubMed: 16366735]
10. Lee WC, et al. A dynamic zone defines interneuron remodeling in the adult neocortex. Proc Natl Acad Sci U S A. 2008; 105:19968–19973. [PubMed: 19066223]
11. Daw NW, Fox K, Sato H, Czepita D. Critical period for monocular deprivation in the cat visual cortex. J Neurophysiol. 1992; 67:197–202. [PubMed: 1552319]
12. LeVay S, Wiesel TN, Hubel DH. The development of ocular dominance columns in normal and visually deprived monkeys. J Comp Neurol. 1980; 191:1–51. [PubMed: 6772696]
13. Hirsch JA, Gilbert CD. Long-term changes in synaptic strength along specific intrinsic pathways in the cat visual cortex. J Physiol. 1993; 461:247–262. [PubMed: 8350264]
14. Frenkel MY, et al. Instructive effect of visual experience in mouse visual cortex. Neuron. 2006; 51:339–349. [PubMed: 16880128]
15. Hofer SB, Mrsic-Flogel TD, Bonhoeffer T, Hubener M. Prior experience enhances plasticity in adult visual cortex. Nat Neurosci. 2006; 9:127–132. [PubMed: 16327785]
16. Hofer SB, Mrsic-Flogel TD, Bonhoeffer T, Hubener M. Experience leaves a lasting structural trace in cortical circuits. Nature. 2009; 457:313–317. [PubMed: 19005470]
17. Sato M, Stryker MP. Distinctive features of adult ocular dominance plasticity. J Neurosci. 2008; 28:10278–10286. [PubMed: 18842887]
18. Sawtell NB, et al. NMDA receptor-dependent ocular dominance plasticity in adult visual cortex. Neuron. 2003; 38:977–985. [PubMed: 12818182]
19. Kameyama K, et al. Difference in binocularity and ocular dominance plasticity between GABAergic and excitatory cortical neurons. J Neurosci. 2010; 30:1551–1559. [PubMed: 20107082]
20. Nassi JJ, Callaway EM. Parallel processing strategies of the primate visual system. Nat Rev Neurosci. 2009; 10:360–372. [PubMed: 19352403]
21. Bullier J, Hupe JM, James AC, Girard P. The role of feedback connections in shaping the responses of visual cortical neurons. Prog Brain Res. 2001; 134:193–204. [PubMed: 11702544]
22. Maunsell JH, van Essen DC. The connections of the middle temporal visual area (MT) and their relationship to a cortical hierarchy in the macaque monkey. J Neurosci. 1983; 3:2563–2586. [PubMed: 6655500]
23. Antonini A, Fagiolini M, Stryker MP. Anatomical correlates of functional plasticity in mouse visual cortex. J Neurosci. 1999; 19:4388–4406. [PubMed: 10341241]
24. Dong H, Shao Z, Nerbonne JM, Burkhalter A. Differential depression of inhibitory synaptic responses in feedforward and feedback circuits between different areas of mouse visual cortex. J Comp Neurol. 2004; 475:361–373. [PubMed: 15221951]
25. Yamashita A, Valkova K, Gonchar Y, Burkhalter A. Rearrangement of synaptic connections with inhibitory neurons in developing mouse visual cortex. J Comp Neurol. 2003; 464:426–437. [PubMed: 12900914]
26. Frenkel MY, Bear MF. How monocular deprivation shifts ocular dominance in visual cortex of young mice. Neuron. 2004; 44:917–923. [PubMed: 15603735]

27. Gordon JA, Stryker MP. Experience-dependent plasticity of binocular responses in the primary visual cortex of the mouse. J Neurosci. 1996; 16:3274–3286. [PubMed: 8627365]
28. Wiesel TN, Hubel DH. Comparison of the effects of unilateral and bilateral eye closure on cortical unit responses in kittens. J Neurophysiol. 1965; 28:1029–1040. [PubMed: 5883730]
29. Silberberg G, Grillner S, LeBeau FE, Maex R, Markram H. Synaptic pathways in neural microcircuits. Trends Neurosci. 2005; 28:541–551. [PubMed: 16122815]
30. Chaudhry FA, et al. The vesicular GABA transporter, VGAT, localizes to synaptic vesicles in sets of glycinergic as well as GABAergic neurons. J Neurosci. 1998; 18:9733–9750. [PubMed: 9822734]
31. Froemke RC, Merzenich MM, Schreiner CE. A synaptic memory trace for cortical receptive field plasticity. Nature. 2007; 450:425–429. [PubMed: 18004384]
32. Gandhi SP, Yanagawa Y, Stryker MP. Delayed plasticity of inhibitory neurons in developing visual cortex. Proc Natl Acad Sci U S A. 2008; 105:16797–16802. [PubMed: 18940923]
33. Markram H, et al. Interneurons of the neocortical inhibitory system. Nat Rev Neurosci. 2004; 5:793–807. [PubMed: 15378039]
34. Buhl EH, et al. Effect, number and location of synapses made by single pyramidal cells onto aspiny interneurones of cat visual cortex. J Physiol. 1997; 500(Pt 3):689–713. [PubMed: 9161986]
35. Kaiser KM, Lubke J, Zilberter Y, Sakmann B. Postsynaptic calcium influx at single synaptic contacts between pyramidal neurons and bitufted interneurons in layer 2/3 of rat neocortex is enhanced by backpropagating action potentials. J Neurosci. 2004; 24:1319–1329. [PubMed: 14960603]
36. Chklovskii DB, Mel BW, Svoboda K. Cortical rewiring and information storage. Nature. 2004; 431:782–788. [PubMed: 15483599]
37. Stepanyants A, Hof PR, Chklovskii DB. Geometry and structural plasticity of synaptic connectivity. Neuron. 2002; 34:275–288. [PubMed: 11970869]
38. Hendry SH, Fuchs J, deBlas AL, Jones EG. Distribution and plasticity of immunocytochemically localized GABAA receptors in adult monkey visual cortex. J Neurosci. 1990; 10:2438–2450. [PubMed: 2165524]
39. Hendry SH, et al. GABAA receptor subunit immunoreactivity in primate visual cortex: distribution in macaques and humans and regulation by visual input in adulthood. J Neurosci. 1994; 14:2383–2401. [PubMed: 8158275]
40. Hendry SH, Jones EG. Reduction in number of immunostained GABAergic neurones in deprived-eye dominance columns of monkey area 17. Nature. 1986; 320:750–753. [PubMed: 3703001]
41. Hendry SH, Jones EG. Activity-dependent regulation of GABA expression in the visual cortex of adult monkeys. Neuron. 1988; 1:701–712. [PubMed: 3272185]
42. Dan Y, Poo MM. Spike timing-dependent plasticity of neural circuits. Neuron. 2004; 44:23–30. [PubMed: 15450157]
43. Hanover JL, Huang ZJ, Tonegawa S, Stryker MP. Brain-derived neurotrophic factor overexpression induces precocious critical period in mouse visual cortex. J Neurosci. 1999; 19:RC40. [PubMed: 10559430]
44. Hensch TK, et al. Local GABA circuit control of experience-dependent plasticity in developing visual cortex. Science. 1998; 282:1504–1508. [PubMed: 9822384]
45. Huang ZJ, et al. BDNF regulates the maturation of inhibition and the critical period of plasticity in mouse visual cortex. Cell. 1999; 98:739–755. [PubMed: 10499792]
46. Kalatsky VA, Stryker MP. New paradigm for optical imaging: temporally encoded maps of intrinsic signal. Neuron. 2003; 38:529–545. [PubMed: 12765606]
47. Chattopadhyaya B, et al. Experience and activity-dependent maturation of perisomatic GABAergic innervation in primary visual cortex during a postnatal critical period. J Neurosci. 2004; 24:9598–9611. [PubMed: 15509747]
48. Kubota Y, Hatada SN, Kawaguchi Y. Important factors for the three-dimensional reconstruction of neuronal structures from serial ultrathin sections. Front Neural Circuits. 2009; 3:4. [PubMed: 19521546]

49. De Paola V, et al. Cell type-specific structural plasticity of axonal branches and boutons in the adult neocortex. Neuron. 2006; 49:861–875. [PubMed: 16543134]

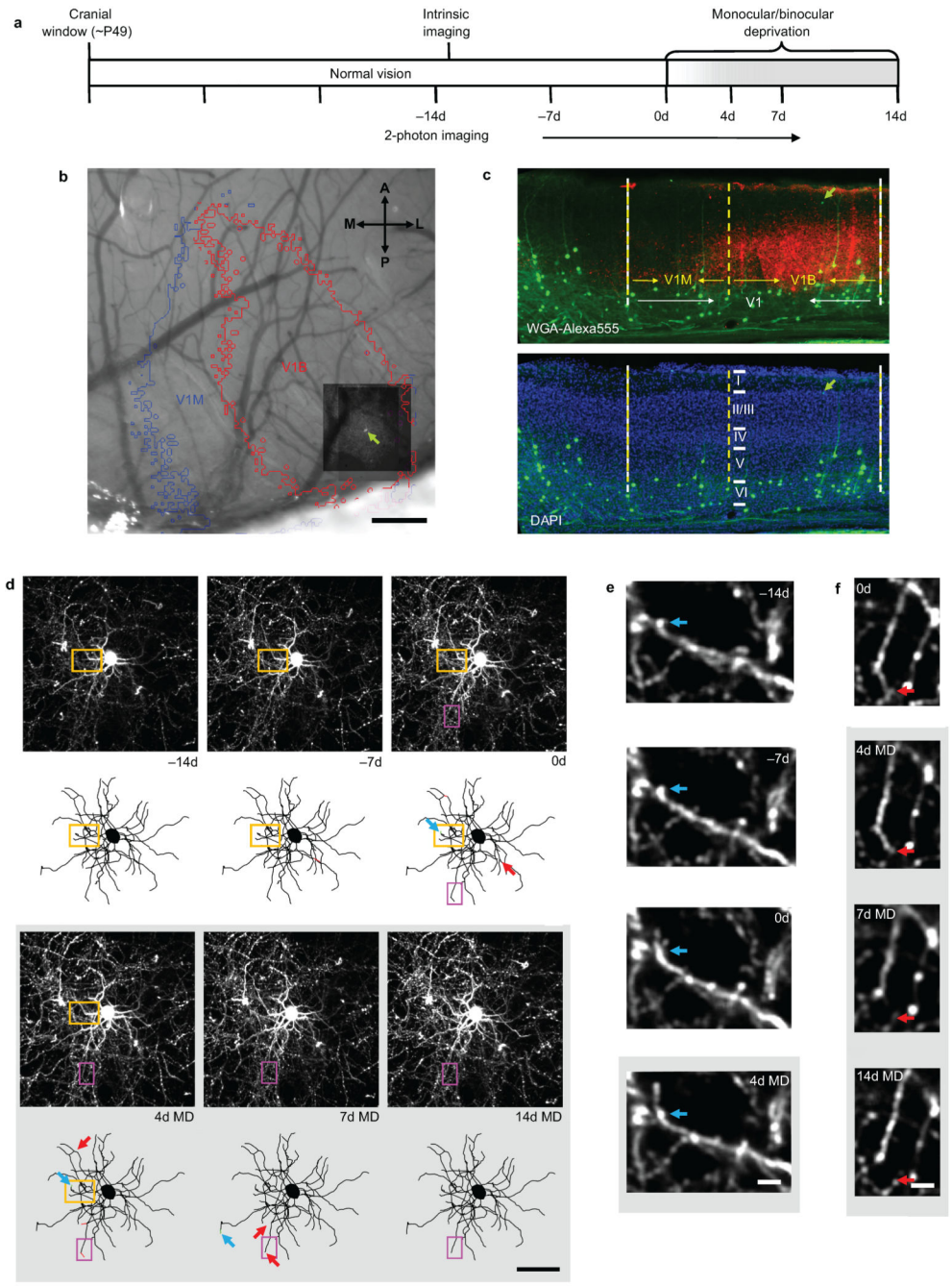

Figure 1.

Chronic two-photon *in vivo* imaging of dendritic branch tip dynamics in superficial L2/3 cortical interneurons. (a) Experimental time course. Every cell was imaged at all time points. (b) Maximum z-projection (MZP) of chronically imaged interneuron (green arrow) superimposed over intrinsic signal map of monocular (V1M) and binocular (V1B) visual cortex. (c) Coronal section of primary visual cortex (V1) containing an imaged superficial L2/3 interneuron (~70 μm below the pial surface) (green arrow) shown with respect to V1M and V1B as identified through WGA-Alexa555 labeling of thalamacortical projections from

the ipsilateral eye (red) and DAPI staining of the granule cell layer (blue). (d) MZPs near the cell body (above) along with two-dimensional projections of three-dimensional skeletal reconstructions (below) of a superficial L2/3 interneuron (~85 μm below the pial surface) in V1B acquired at the specified intervals. Dendritic branch tip elongations and retractions identified between successive imaging sessions are indicated by green and red arrows, respectively. (e) High-magnification view of one branch tip elongation (orange box in [d]). Blue arrow marks the approximate distal end of the branch tip at −14d. (f) High-magnification view of one branch tip retraction (magenta box in [d]). Red arrow marks the approximate distal end of the branch tip at 0d. Scale bars: (b), 250 μm; (c), 100 μm; (d), 50 μm; (e,f), 5 μm.

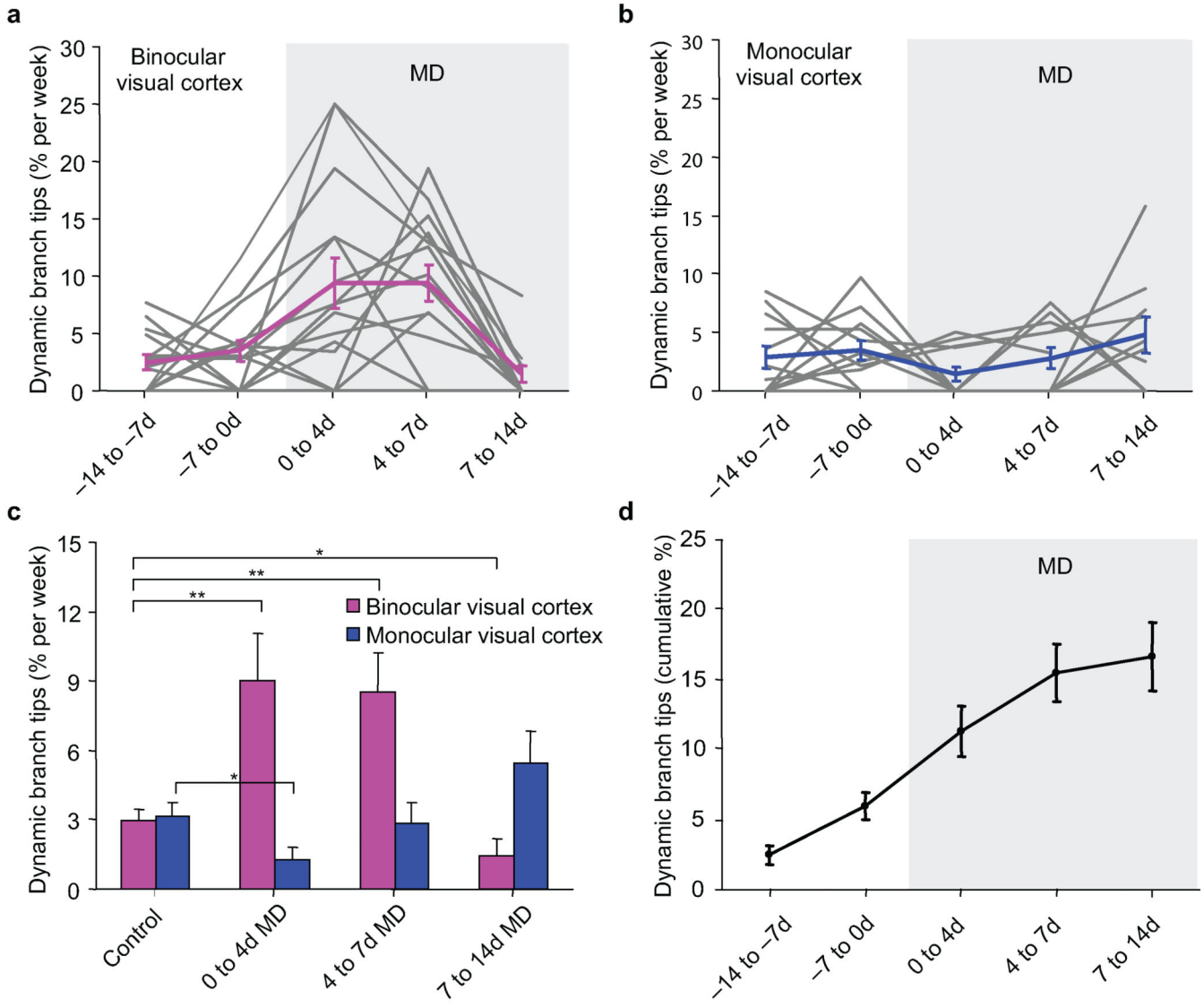

Figure 2.

Monocular deprivation increases interneuron dendritic branch tip dynamics in adult binocular visual cortex. (a,b) Dendritic branch tip dynamics in superficial L2/3 interneurons imaged throughout a 14 day monocular deprivation for: (a) binocular visual cortex, individual cells shown in grey, mean shown in magenta. (n = 16 cells from 13 mice, 524 branch tips) and; (b) monocular visual cortex, individual cells shown in grey, mean shown in blue. (n = 12 cells from 12 mice, 461 branch tips). (c) Rate of dendritic branch tip dynamics compared before and during monocular deprivation in binocular (magenta) and monocular (blue) visual cortex. (d) Cumulative fraction of dynamic branch tips in binocular visual cortex over imaging time course. (** $p < 0.01$, * $p < 0.05$). Error bars, s.e.m.

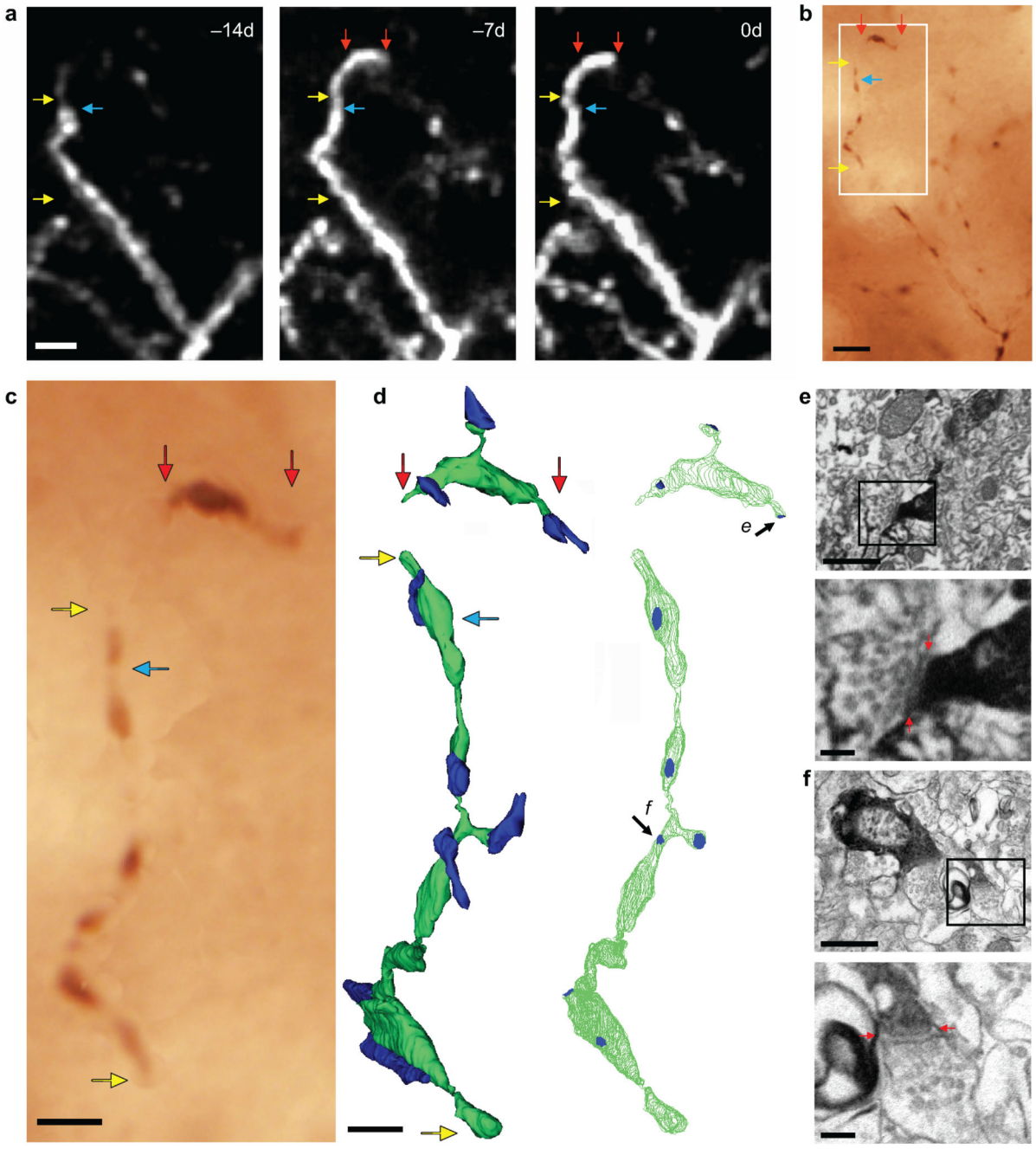

Figure 3.

Synapses are formed on newly extended branch tips. (a) *In vivo* image of a branch tip elongation. Blue arrow marks the approximate distal end of the branch tip at −14d. (b) Re-identification of the same imaged dendrite in fixed tissue following immuno-staining for GFP. (c) High-magnification view of dendritic portion reconstructed by serial section electron microscopy (white box in [b]). (d) Serial section electron microscopy reconstruction of the *in vivo* imaged dendrite (in green) with region proximal to (yellow arrows in a-c) and very distal portion of (red arrows in a-c) elongated branch tip. Left panel indicates

contacting axon terminals (in blue). Right panel indicates synaptic contacts (in blue). (e, f) Electron micrographs showing a synapse on the newly elongated branch tip (*e* arrow in [d]) and on the proximal, stable dendrite (*f* arrow in [d]), respectively. Bottom panels show an enlargement of the synapse with visible synaptic cleft (red arrows) and synaptic vesicles. Scale bars: (a,b), 5 μm; (c), 2μm; (d), 1 μm; (e,f – top panels), 500 nm; (e,f – bottom panels), 100 nm.

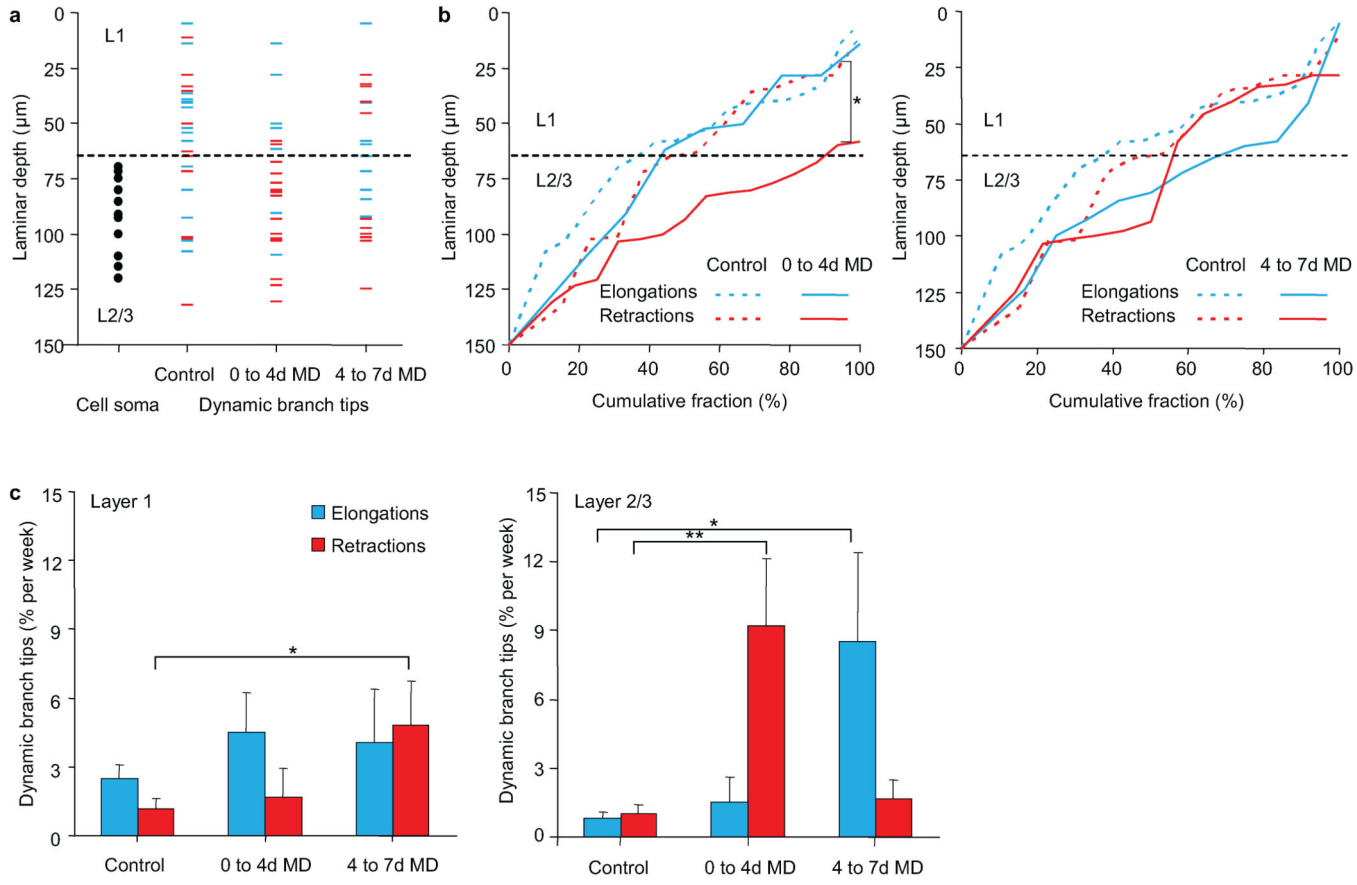

Figure 4.

Monocular deprivation induces laminar specific dendritic arbor rearrangements. (a) Distribution of dynamic branch tips before and during monocular deprivation in binocular visual cortex. Plotted are cell soma positions (black circles) and branch tips positions of branch tip elongations (blue) or retractions (red). (b) Cumulative fraction distribution plot of branch tip elongations (blue) and retractions (red) at 0–4d MD (left) and 4–7d MD (right) as compared to control (dotted lines) (* $p < 0.05$). (c) Rate of dendritic branch tip elongations (blue) and retractions (red) in L1 and L2/3 of binocular visual cortex, before and during monocular deprivation. (n = 16 cells from 13 mice, L1: 228 branch tips. L2/3: 325 branch tips) (** $p < 0.01$, *$p < 0.05$). Error bars, s.e.m.

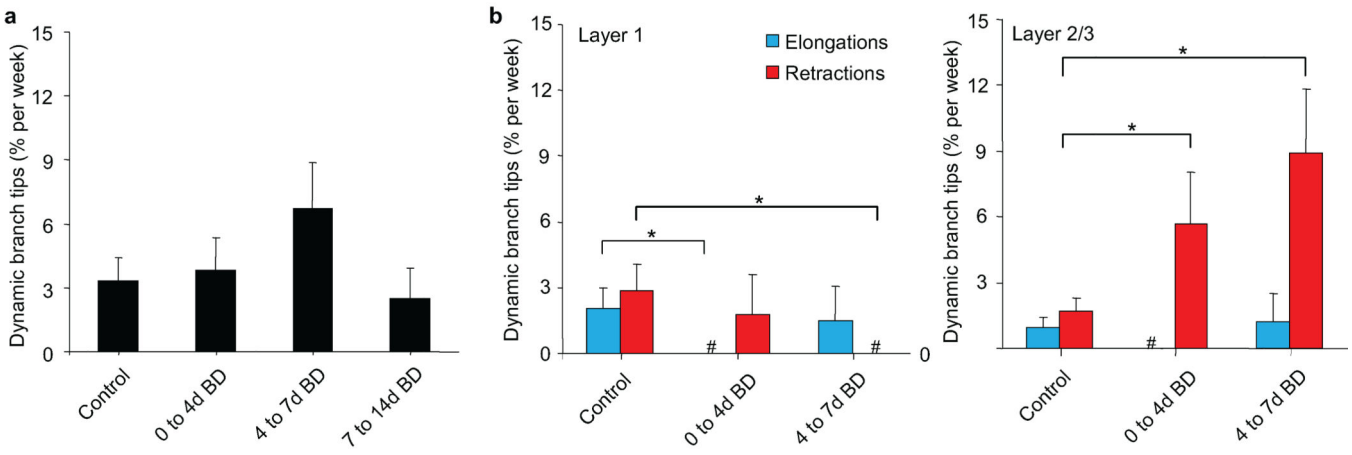

Figure 5.

Binocular deprivation specifically increases retractions of L2/3 branch tips. (a) Dendritic branch tip dynamics compared before and during binocular deprivation in binocular visual cortex. (b) Rate of branch tip elongations (blue) and retractions (red) in L1 and L2/3 of binocular visual cortex, before and during binocular deprivation. (n = 7 cells from 7 mice, L1: 108 branch tips. L2/3: 155 branch tips) (# denotes a time point measurement equaling 0 ± 0.00 % dynamic branch tips / wk) (** $p < 0.02$, * $p < 0.05$). Error bars, s.e.m.

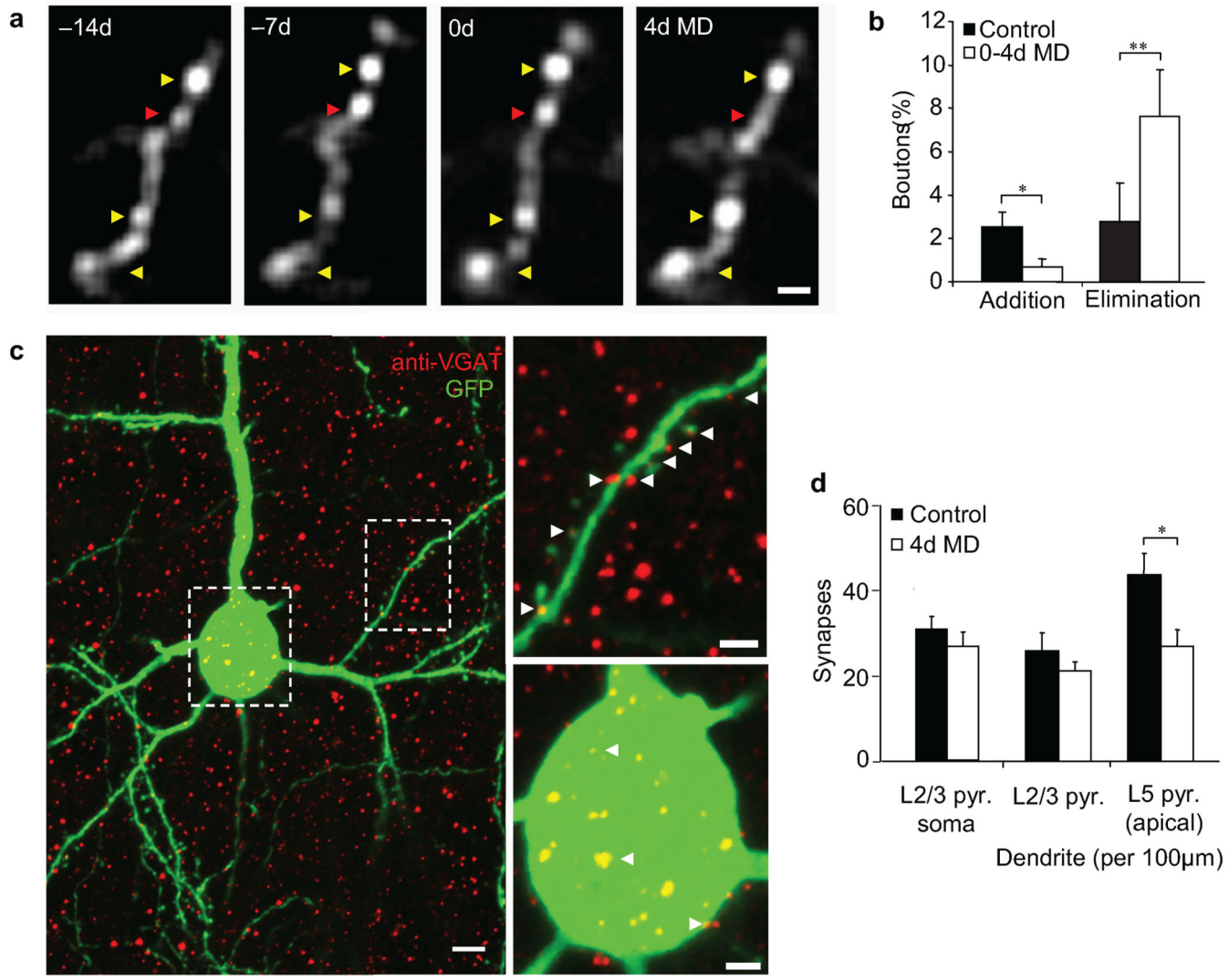

Figure 6.

Early period of monocular deprivation increases inhibitory synapse elimination onto L5 pyramidal apical dendrites. (a) High-magnification view of axonal bouton remodeling of superficial L2/3 interneuron. Yellow arrow indicates stable boutons. Red arrow indicates an eliminated bouton. (b) Fraction of total axonal boutons added or eliminated during normal vision or in response to 4 days of monocular deprivation. (n = 6 cells from 6 mice, 564 axonal boutons) (** $p < 0.01$, *$p < 0.05$). (c) Coronal section of a GFP-labeled L2/3 pyramidal neuron in binocular visual cortex (in green) after immunohistochemical staining of inhibitory pre-synaptic terminals by VGAT (in red). Examples of inhibitory presynaptic contacts onto dendritic (top-right panel) and perisomatic (bottom-right panel) synapses are indicated with white arrows. (d) Quantification of putative inhibitory synapse density on L2/3 pyramidal neuron soma and on dendrites of L2/3 and L5 pyramidal neurons in binocular visual cortex after four days of monocular deprivation. (control; n=8 mice, 49 L2/3 pyramidal neurons, 45 L5 pyramid neurons, 9688 synapses, 4d monocular deprivation n = 8, 46 L2/3 pyramidal neurons, 39 L5 pyramid neurons, 8581 synapses) (*$p < 0.05$).

Error bars, s.e.m. Scale bars: (a, c - top-right, c -bottom-left panel), 2 μm; (c - left panel), 5 μm.

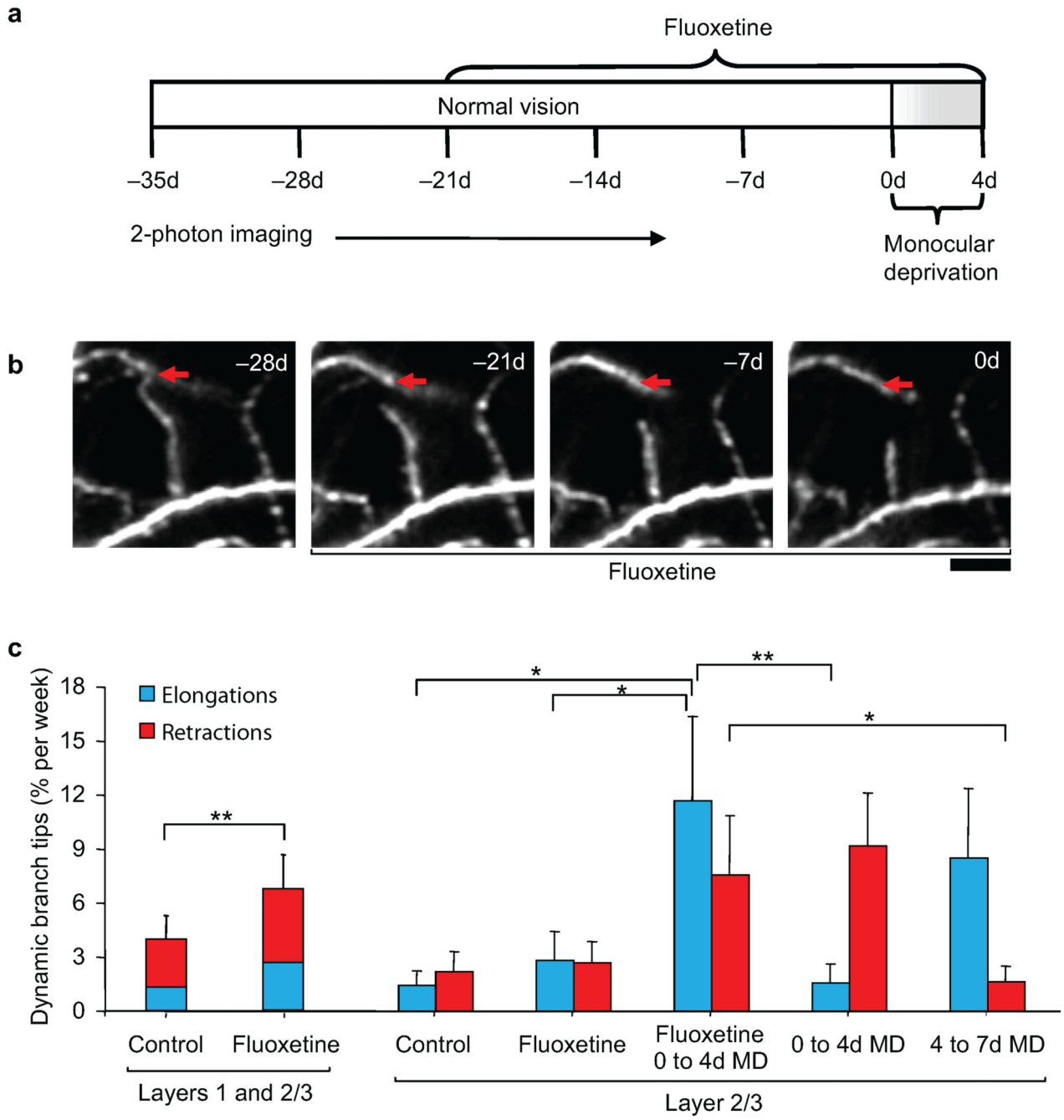

Figure 7.

Reduction in intracortical inhibition by fluoxetine treatment promotes experience-dependent branch tip remodeling. (a) Experimental time course. (b) High-magnification view of one branch tip retraction during fluoxetine treatment. Red arrow marks the approximate distal end of the branch tip at −28d. Scale bar: 10 μm. (c) Dendritic branch tip dynamics in L1 and L2/3 of binocular visual cortex of animals under normal vision before and during fluoxetine administration. Rates of L2/3 branch tip elongations and retractions in binocular visual cortex during fluoxetine treatment under normal vision or a brief 4d monocular deprivation

as compared to prolonged 7d monocular deprivation without fluoxetine treatment (taken from Fig 4c.) (with fluoxetine, n = 8 cells from 8 mice, L1: 113 branch tips, L2/3: 115 branch tips; without fluoxetine, n = 16 cells from 13 mice, L2/3: 325 branch tips). (** $p < 0.01$; * $p < 0.05$). Error bars, s.e.m.